JACS
JOURNAL OF THE AMERICAN CHEMICAL SOCIETY

Article

A Mitochondria-Specific Fluorescent Probe for Visualizing Endogenous Hydrogen Cyanide Fluctuations in Neurons

Lingliang Long, Meiyu Huang, Ning Wang, yanjun wu, kun wang, Aihua Gong, zhijian zhang, and Jonathan L. Sessler

J. Am. Chem. Soc., **Just Accepted Manuscript** • DOI: 10.1021/jacs.7b12545 • Publication Date (Web): 16 Jan 2018

Just Accepted

ACS Publications

Journal of the American Chemical Society is published by the American Chemical Society. 1155 Sixteenth Street N.W., Washington, DC 20036

A Mitochondria-Specific Fluorescent Probe for Visualizing Endogenous Hydrogen Cyanide Fluctuations in Neurons

Lingliang Long,[†,‡] Meiyu Huang,[‡] Ning Wang,[‡] Yanjun Wu,[‡] Kun Wang,[‡] Aihua Gong,[§] Zhijian Zhang,[§] Jonathan L. Sessler[*,†]

†Department of Chemistry, The University of Texas at Austin, 105 East 24th Street, Stop A5300, Austin, Texas 78712-1224, United States

‡Scientific Research Academy & School of Chemistry and Chemical Engineering, Jiangsu University, Zhenjiang, Jiangsu 212013, P. R. China.

§School of Medicine, Jiangsu University, Zhenjiang, Jiangsu 212013, P. R. China

Supporting Information Placeholder

ABSTRACT: An ability to visualize HCN in mitochondria in real time may permit additional insights into the critical toxicological and physiological roles this classic toxin plays in living organisms. Herein, we report a mitochondria-specific coumarin pyrrolidinium-derived fluorescence probe (**MRP1**) that permits the real time ratiometric imaging of HCN in living cells. The response is specific, sensitive (detection limit is ca. 65.6 nM), rapid (within 1 s), and reversible. Probe **MRP1** contains a benzyl chloride subunit designed to enhance retention within the mitochondria under conditions where the mitochondria membrane potential is eliminated. It has proved effective in visualizing different concentrations of exogenous HCN in the mitochondria of HepG2 cells, as well as the imaging of endogenous HCN in the mitochondria of PC12 cells and within neurons. Fluctuations in HCN levels arising from the intracellular generation of HCN could be readily detected.

INTRODUCTION

The cyanide anion (CN^-) is a recognized toxin.[1] For humans blood cyanide levels higher than 20 μM are considered toxic.[2] However, cyanide is widespread in the modern world, and cyanide exposure from gold mining, electroplating, metallurgy,[3a] consumption of certain foods,[3b] bacterial cyanogenesis,[3c] uncontrolled fires,[3d] cigarette smoke,[3e] vehicle exhaust,[3f] and from pharmaceutical by-products,[3g] are potential concerns. At the subcellular level, the mitochondria are recognized as being the primary site of cyanide toxicity. This is because cyanide inactivates mitochondrial cytochrome C oxidase and halts cellular respiration.[4] It also induces production of reactive oxygen species, including hydroxyl radicals (·OH) within mitochondria.[5] This leads to the oxidative damage to mitochondrial DNA and further results in mitochondrial dysfunction. This dysfunction is linked to a variety of diseases, including Alzheimer's disease,[6a] Huntington's disease,[6b] Parkinson's disease,[6c] Diabetes,[6d] and cancer.[6e]

On the other hand, despite its high toxicity, growing evidence suggests that the cyanide anion is generated in specific cells and plays important physiological roles within the human body.[7-9] At the physiological pH of 7.4, cyanide exists predominantly as hydrogen cyanide (HCN) due to its pKa value of 9.3. In leukocytes, HCN is produced by the myeloperoxidase-mediated oxidative chlorination of glycine or N-terminal glycyl peptides during phagocytosis, and is used as a defense against bacteria, fungi, and other pathogens.[7] It has also been suggested that HCN is generated within neurons upon the activation of opioid receptors by endogenous or exogenous opioids.[8] The HCN generated in this way has been proposed as a novel neuromodulator within the central and peripheral nervous system in loose analogy to nitric monoxide (NO), carbon monoxide (CO), and hydrogen sulfide (H_2S).[9] Unfortunately, experimental support for the putative role of HCN in neurons remains elusive. Mitochondria have been suggested as being the main locus for the production of HCN within the neurons;[8c] however, this is far from established. Effective HCN probes that operate within mitochondria may allow deeper insights into the critical toxicological and physiological roles of HCN within living organisms. As detailed below, we have now prepared a probe that appears promising in this regard.

Fluorescent probes have received considerable attention due to the high sensitivity, fast response time, technical simplicity, and applicability to biological milieus.[10] In combination with laser scanning confocal microscope (LSCM), appropriately designed fluorescent probes can be used to sense important species in subcellular organelles in a non-invasive manner.[11] Currently, a large number of fluorescent probes for cyanide are known. As a general rule, these systems rely on the unique nucleophilic reactivity of the cyanide anion to trigger a change in the fluorescent response.[12] Fluorescent probes for the cyanide anion that are based on its interactions with metal ions,[13] H^+,[14] and boronic acid derivatives[15] are also known. To date, cyanide anion probes have been used to sense endogenous cyanide in plant samples.[13a, 16] However, to our knowledge, no cyanide anion probe has been used successfully to monitor endogenous HCN levels in mitochondria.

To be effective at the mitochondrial level, we suggest that a fluorescent HCN probe needs to meet the following prerequisites: (a) It should display a fast response upon exposure to HCN. (b) Give rise to a so-called ratiometric output so as to reduce potential artifacts associated with, e.g., photobleaching, probe distribution, or changes in excitation intensity.[17] (c) The induced changes should be reversible so as to allow fluctuations in HCN levels in cells and organelles to be monitored in real time. (d) Possess a

high inherent fluorescence quantum yield (Φ_f) and be effective at low concentrations (25-500 nM). (e) Be retained in the mitochondria when the mitochondria membrane potential is eliminated. The latter requirement is particularly germane to the design of an HCN probe. The negative mitochondrial membrane potential ($\Delta\psi$) typically allows the targeting of positively charged species to the mitochondria.[11] However, high concentrations of HCN can lead to a loss in the mitochondrial membrane potential,[18] leading to diffusion of erstwhile targeted species into the cytoplasm. In such instances, the further study of mitochondria-related changes in HCN concentrations would be precluded.

RESULTS AND DISCUSSION

Rational design of the Probe

Bearing the above considerations in mind, a ratiometric fluorescent probe for visualizing HCN within the mitochondria of living cells was designed as shown in Scheme 1a. Full synthetic details are provided in the Supporting Information. A 7-diethylamino-coumarin dye (green color) was selected as the fluorophore while a 1-methylenepyrrolidinium subunit (pink color) was used as the reactivity-based recognition site for HCN. In preliminary studies, we found that the 1-methylenepyrrolidinium group can rapidly, specifically, and reversibly react with HCN. By tethering a 7-diethylamino-coumarin moiety to the 1-methylenepyrrolidinium subunit through an ethylene linker, we expected to have a system that would give rise to a ratiometric fluorescence response to HCN as the result of modulating the intramolecular charge transfer (ICT)[19] interactions between the electron donating coumarin and electron withdrawing pyrrolidinium groups (referred to as EDG and EWG, respectively). Perturbing the ICT interactions between linked EDG and EWGs can have a significant effect on the fluorescence emission.[20,21] In an effort to study this effect in the present instance and optimize the fluorescence quantum yield of the probe, a 4-substituted phenyl group (blue color) was tethered to the electron deficient 1-methylenepyrrolidinium group. We hypothesized that changing the substituents at the 4-position of the phenyl group might allow the extent of the ICT interaction to be fine-tuned. Thus compounds **1a**-**1e** with different electron donating or electron withdrawing substituents at the 4-position of the appended phenyl group were designed and synthesized (Scheme 1a). Predicative studies of these HCN probes, discussed below, then allowed for the preparation of a mitochondrial probe, **MRP1**, suitable for use as in vitro.

As a first step towards understanding the HCN response function of compounds **1a**-**1e**, their optical properties were investigated (Fig. S1, Table S1). Compound **1a** exhibited a dominant absorption feature centered at 521 nm, which is ascribed to an ICT transition. In the case of the systems bearing electron withdrawing substituents (Cl, CN) at the 4-position of the phenyl group, i.e., **1d** and **1e**, slightly red-shift absorption bands were observed at 524 and 530 nm, respectively. In contrast, more substantial blue shifts were seen upon the introduction of electron donating groups (i.e., OH, diethylamino); in fact, absorption features at 515 nm and 513 nm were seen for compounds **1b** and **1c,** respectively.

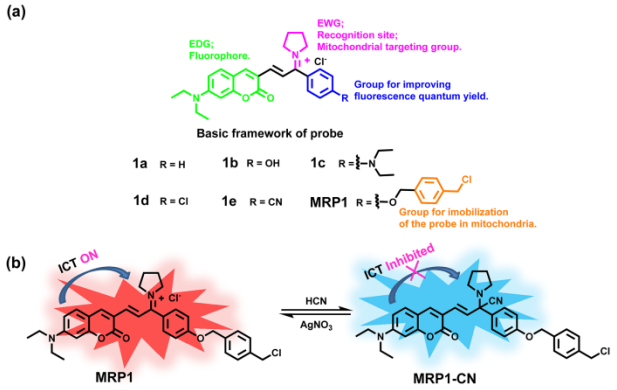

Scheme 1. (a) Components making up the present series of HCN probes. Note that different substituent are present at the 4-position of the phenyl group; (b) proposed basis for the sensing response of **MRP1** and related HCN probes.

Upon excitation at 521 nm, compound **1a** displayed a fluorescence emission band centered at 602 nm with an associated quantum yield (Φ_f) of 0.184 (Fig. S1b, Table S1). Compared to **1a**, the fluorescence quantum yields of **1d** (Φ_f = 0.166) and **1e** (Φ_f = 0.062) were reduced. In contrast, compound **1b**, had a higher fluorescence quantum yield (Φ_f = 0.285). On the other hand, compound **1c** displayed little appreciable fluorescence intensity (Φ_f = 0.002).

To obtain insights into the optical properties of compounds **1a**-**1e**, time-dependent density functional theory (TD-DFT) calculations were carried out. The electron densities in the HOMO and LUMO of these compounds in the ground state and first excited singlet state are shown in Fig. S2. On the basis, it is concluded that the HOMO→ LUMO transitions for compound **1a**, **1b**, **1d**, and **1e** involve electron density redistributions from the EDG to EWG. In other words, ICT is predicated upon excitation. In stark contrast, in the first excited singlet state of compound **1c**, the HOMO→ LUMO transition involves an electron density redistribution from the 4-diethylamino-phenyl group to the 7-diethylaminocoumarin moiety, which acts as an electron acceptor, not donor.

The dihedral angles between the 7-diethylamino-coumarin ring and the 4-substituted phenyl ring of compound **1a**-**1e** in the optimized geometry are given in Table S2 and Fig. S3. In the ground state (S_0), the dihedral angles between the coumarin ring and the phenyl ring in compounds **1a**, **1b**, **1d**, and **1e** were approximately 60°. In the first excited singlet state (S_1) these dihedral angles decrease to around 50°. The dihedral angle of compound **1c** in its ground (S_0) state is 57°, which is similar to that calculated for **1a**, **1b**, **1d**, and **1e**. Whereas in the S_1 state, the corresponding dihedral angle for **1c** increases to 88°. It was also found that the fluorescence intensity of **1c** increases with increasing solvent viscosity (Fig S4). Taken in concert, these findings lead us to suggest that the fluorescence quenching of compound **1c** is best ascribed to a twisted intramolecular charge transfer (TICT)[22] from the 4-diethylamino phenyl group to the 7-diethylamino-coumarin.

The charge transfer process underlying the presumed ICT may be described in terms of the charge transfer parameter f_{CT} $=\Delta q_D - \Delta q_A$, where Δq_D and Δq_A denote the changes in the charge of the donor and the acceptor, respectively, upon excitation from the ground state to the lowest excited state.[23] As shown in Table S3, in the S_1 state, compound **1a** has f_{CT} around 0.45. By varying the substituents, the f_{CT} value could be increased to 0.57 in the case of **1e**. Likewise, it decreases to about 0.39 in **1b**. Thus, the ICT strength can be fine-tuned by varying the substituents at the 4-position of the phenyl group.

Compound **1b** displayed the highest fluorescence quantum yield within the series **1a**-**1e**. The key *para*-oxygen atom was thus retained in designing a putative ratiometric fluorescent probe for HCN, namely **MRP1** (Scheme 1a). Probe **MRP1** differs from **1b** in that an additional benzyl chloride group (orange color) is incorporated into the framework. This group can react with free thiol groups present in mitochondrial proteins and thus serve potentially to immobilize the probe within mitochondria, even in instances when the mitochondria membrane potential is eliminated.[24]

Spectral response of probe MRP1 to HCN

The ability of probe **MRP1** to react with HCN was evaluated in 20 mM potassium phosphate buffer/acetonitrile (pH 7.4, 1:3 v/v) at room temperature. In its free form, probe **MRP1** exhibited a fluorescence emission feature centered at 599 nm (Φ_f = 0.261) under these conditions. Upon addition of cyanide (as its KCN salt), the fluorescence emission of **MRP1** at 599 nm gradually decreased while a new emission feature at 490 nm was seen to grow in (Fig. 1a). An isoemission point was clearly visible at 552 nm during this addition process. The emission ratio (I_{490}/I_{599}), an indicator of a ratiometric response, was found to be linearly proportional to the concentration of cyanide anion over the 0-35 μM concentration range (Fig. S5). Based on a signal-to-noise (S N^{-1}) ratio of 3, a detection limit of 65.6 nM was calculated; this is much lower than the concentration of HCN typically found in the brain of healthy individuals (2-10 μM).[9b] The absorption maximum of probe **MRP1** was also found to undergo a blue shift (from 516 nm to 411 nm) upon treatment with cyanide (Fig S6). The ratiometric fluorescence response of **MRP1** to cyanide was also evaluated at different pH values. On the basis of the results obtained (cf. Fig. S7) it is concluded that **MRP1** can be used to detect cyanide over the pH 5–8 range. The stability of **MRP1** in aqueous solution was tested by means of fluorescence spectral analyses. In various mixtures of acetonitrile and buffer, no change in the fluorescence signature was seen over the course of 24 h, leading us to infer that **MRP1** is stable over at least such a time scale (Fig. S8). The effect of the relative concentration of CH_3CN was also investigated (Fig. S9); on this basis, it was determined that **MRP1** can be used to sense cyanide even in aqueous solutions containing only 30% acetonitrile.

Time-dependent studies of the fluorescence changes produced when **MRP1** is treated with cyanide revealed a response that occurs within ≤1 s (Fig. 1b). The fast response time is considered beneficial for a probe designed to monitor HCN concentrations in real time. After reacting with cyanide, probe **MRP1** was treated with $AgNO_3$ (Fig. 1c). Sequential additions of cyanide and silver(I) led to a turning off and on of the 599 nm fluorescent feature. On this basis, we conclude that **MRP1** may allow for the reversible monitoring of HCN fluctuations in living cells.

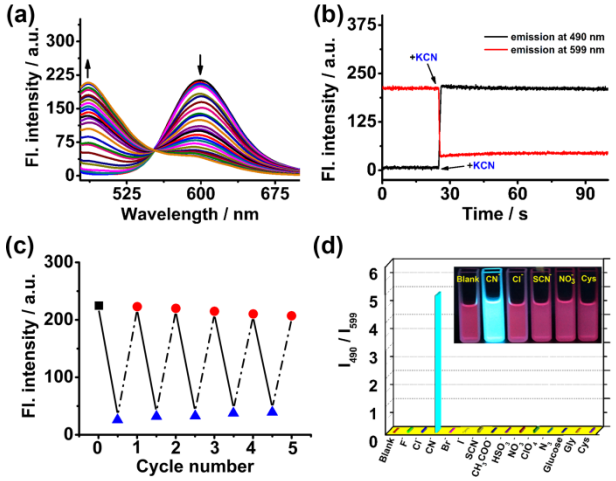

Fig. 1 (a) Changes in the fluorescence emission spectra of **MRP1** (1 μM) seen upon the addition of increasing quantities cyanide (0-60 μM as its KCN salt) at room temperature (λ_{ex} = 467 nm). (b) Time dependent changes in the fluorescence emission intensities recorded at 490 nm and 599 observed upon treatment **MRP1** (1 μM) with cyanide (60 μM). (c) Changes in the fluorescence intensity of **MRP1** (1 μM) seen upon the sequential addition of first cyanide (60 μM) and then $AgNO_3$ (60 μM) (λ_{ex} = 467 nm, λ_{em} = 599 nm); (■) **MRP1**, (▲) **MRP1** + CN^-, (●) **MRP1** + CN^- + $AgNO_3$. (d) Ratiometric fluorescence response of **MRP1** (1 μM) seen upon exposure to 60 μM of various putative analytes. Inset: Photos of **MRP1** (1 μM) taken in the presence of various species (60 μM) under the illumination of a handheld UV lamp. All studies were carried out in 20 mM potassium phosphate buffer/acetonitrile, pH 7.4, 1:3 v/v.

The response of **MRP1** towards other putative analytes was also explored. When **MRP1** (1 μM) was treated with either of other physiologically relevant anions (e.g., F^-, Cl^-, Br^-, I^-, CH_3COO^-, HSO_3^-, NO_3^-, ClO_4^-, and N_3^-; studied as their Na^+, Li^+, or K^+ salts) or typical biological molecules (Glucose, Gly and Cys; all at 60 μM), no significant change was observed in the(I_{490}/I_{599}) emission ratio (Fig. 1d). Only when cyanide was added was a noticeable response observed. This response toward cyanide was retained in the presence of other relevant species, most of which produced no appreciable or only minimal interference (Fig. S10). This selectivity was apparent to the naked eye. Under conditions of illumination using a handheld UV lamp cyanide produced a distinctive color signature with **MRP1** not seen in the case of other putative analytes (Fig. 1d).

Compound **1a** displayed a similar ratiometric fluorescence response to cyanide (Fig S11). However, its structure is much simpler than that of **MRP1**. Therefore, for clarity, compound **1a** was used to investigate the sensing reaction mechanism. The reaction product of **1a** with cyanide was isolated and characterized. As inferred from ^1H NMR and ^{13}C NMR spectral studies and mass spectrometric analyses (Fig. S12 - Fig. S14), the optical response seen in the case of **1a** and by extension **MRP1** reflects the nucleophilic addition of cyanide anion to the 1-methylenepyrrolidinium moiety present in these two congeneric probes. This addition interferes with an efficient ICT from the EDG to the EWG, which, in turn, results in a blue shift in both the emission and absorption spectral features (Scheme 1b). Support for this conclusion came from TD-DFT calculations (Figs. S15 and S16).

Fluorescence imaging of HCN in the mitochondria of living cells

To assess the mitochondrial staining ability of **MRP1**, co-localization experiments were carried out using Mitotracker Deep Red (**MTDR**),[25] a commercially available mitochondrial dye. In these studies, HepG2 cells were co-incubated with **MRP1** (0.5 μM) and **MTDR** (0.5 μM) at 37 °C for 15 min. As can be seen by inspection of Fig. 2c, a clear mitochondria profile with strong near-infrared (NIR) fluorescence was observed in the NIR channel, which was ascribed to **MTDR**. A similar mitochondria profile was observed in the red channel, which is largely reflective of probe **MRP1** (Fig. 2b). The **MRP1** response coincides well with that of **MTDR** (Fig. 2d) as reflected in a Pearson's co-localization coefficient of 0.94. Compound **1b** was also studied and likewise found to display mitochondria-specific staining (Fig. 2e-2h). Considered in concert, these results provide support for the notion that both **MRP1** and **1b** act as organelle specific probes that target the mitochondria.

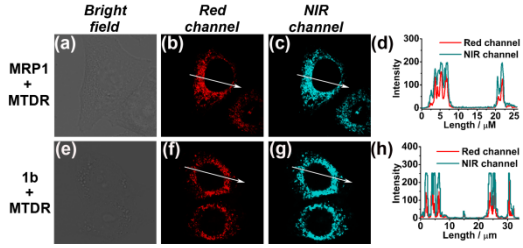

Fig. 2 Confocal image of HepG2 cells co-stained with either **MRP1** and **MTDR** or **1b** and **MTDR**. (a)-(c) Bright field, red (λ_{em} = 575-650 nm) and NIR (λ_{em} = 660-740 nm) images of HepG2 cells co-stained with **MRP1** and **MTDR**. (d) Intensity profile of regions of interest (ROIs) in the co-stained HepG2 cells as indicated by the white arrows in (b) and (c). (e)-(g) Bright field, red and NIR images of HepG2 cells co-stained with **1b** and **MTDR**. (h) Intensity profile of the ROIs indicated in (f) and (g).

To test whether **MRP1** would remain in the mitochondria after the mitochondrial membrane potential was eliminated, the HepG2 cells were stained with **MRP1** and then further incubated with CCCP (carbonyl cyanide *m*-chlorophenyl hydrazone). CCCP is a reagent that can collapse the mitochondrial membrane potential.[26] As inferred from the results summarized in Fig 3, **MRP1** is retained in the mitochondria after co-incubating with CCCP for 80 min. However, after treatment with CCCP, compound **1b** was found to diffuse from the mitochondria into the cytoplasm. The difference between these two dye systems is ascribed to the presence of the benzyl chloride moiety in **MRP1** that, per the design expectations, acts as an immobilizing group.

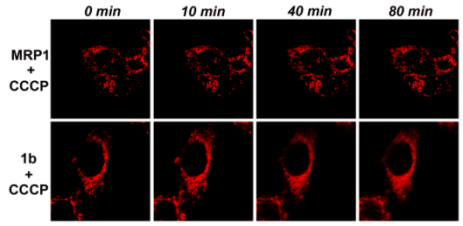

Fig. 3 Confocal images of HepG2 cells stained with **MRP1** (0.5 μM) or **1b** (0.5 μM) in the presence of CCCP (10 μM) and recorded at different time intervals. The images were produced by monitoring the red channel (λ_{em} = 575-650 nm).

Prior to testing **MRP1** as a sensor for endogenous cyanide, its ability to function as ratiometric fluorescence probe for exogenous HCN was examined. It was found that HepG2 cells loaded with **MRP1** alone showed negligible fluorescence in the green channel but a strong fluorescence in the red channel (Fig. 4a-4c). On this basis, it is concluded that negligible quantities of HCN are present in HepG2 cells. After the addition of 15 μM KCN, which is largely transformed to HCN under physiological conditions, the fluorescence seen in the red channel decreased, while that in the green channel increased (Fig. 4d-4f). In the presence of 40 μM cyanide, the fluorescence in the red channel was almost fully quenched, while that of the green channel became commensurately brighter (Fig. 4g-4i). The subsequent addition of cyanide, lead to an increase in green-to-red fluorescence ratio (F_{green} / F_{red}) (Fig 4m). The increase was found to be linearly proportional to the cyanide concentration, leading us to suggest that probe MRP1 is potentially suitable for quantitative studies (Fig. 4n).

To verify that the fluorescence response was due to HCN, the HepG2 cells loaded with cyanide were treated with methemoglobin (MHb; a scavenger of cyanide)[27] to reduce the intracellular levels of HCN. In the presence of MHb, the fluorescence response was significantly inhibited (Fig 4j-4l), as expected for a fluorescence response that is directly correlated to the HCN levels.

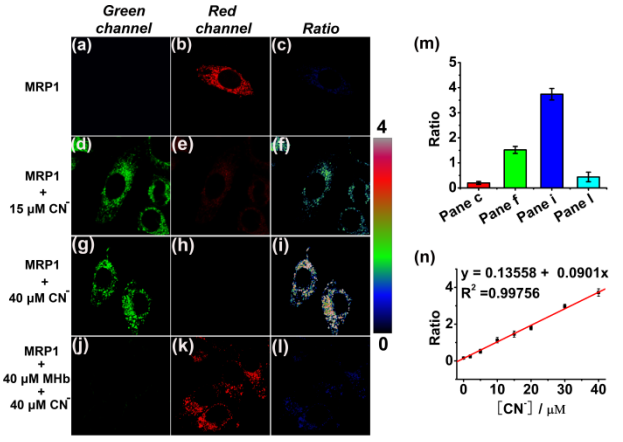

Fig. 4 Confocal images of live HepG2 cells stained with **MRP1** (0.5 μM) in the presence of different concentrations of exogenous cyanide. (a)-(c) Images recorded over the green (λ_{em} = 460-530 nm) and red (λ_{em} = 575-650 nm) channels, and the corresponding (F_{green} / F_{red}) ratio for HepG2 cells stained with **MRP1** cells and incubated with 0 μM cyanide. (d)-(f) Green and red channel and ratiometric imaging of HepG2 cells stained with **MRP1** and incubated with 15 μM cyanide. (g)-(i) Green and red channel and ratiometric imaging of **MRP1** stained HepG2 cells incubated with 40 μM cyanide. (j)-(l) Green and red channel and ratiometric imaging of **MRP1** stained HepG2 cells pretreated with 40 μ M MHb, and then incubated with 40 μ M cyanide. (m) Average intensity ratios from images (c), (f), (i), and (l). (n) Linear relationship between the average intensity ratio and cyanide concentration. Error bars represent the standard deviation.

Next, the potential utility of **MRP1** as a probe for of endogenously generated HCN was evaluated. This was done using rat pheochromocytoma cells (PC12 cells), neuron-like cells that are known to release HCN.[8a] Upon incubation with **MRP1** for 15 min, a strong fluorescence in the green channel (Fig. 5a) and weak fluorescence in the red channel (Fig. 5b) was seen. The fluorescence ratio (Fig. 5c) was enhanced in the case of the PC12 cells as compared to what was seen with HepG2 cells (cf. Fig. 4c). Based

on the fluorescence ratio and the equation given in Fig 4n, the response in the PC12 cells was equivalent to that seen when the HepG2 cells were treated with 8.1 μM cyanide.

Hydromorphine (HYDROM) is a type of μ-opiate agonist that can stimulate nerve cells to produce HCN.[8a] After treatment with 10 μM HYDROM for 15 min, the fluorescence ratio seen in the case of the PC12 cells was further enhanced. In this case, the endogenous HCN concentration was calculated to be 23.0 μM. On the other hand, pretreatment of the PC12 cells with 40 μM MHb (to remove the endogenous HCN) followed by incubatation with **MRP1** for 15 min led to little if any fluorescence being observed in the green channel (Fig. 5g). However, under these conditions a strong fluorescence response was seen in the red channel (Fig. 5h). The fluorescence ratio was reduced significantly (Fig. 5i, 5j), and the HCN concentration was calculated to be only 0.2 μM.

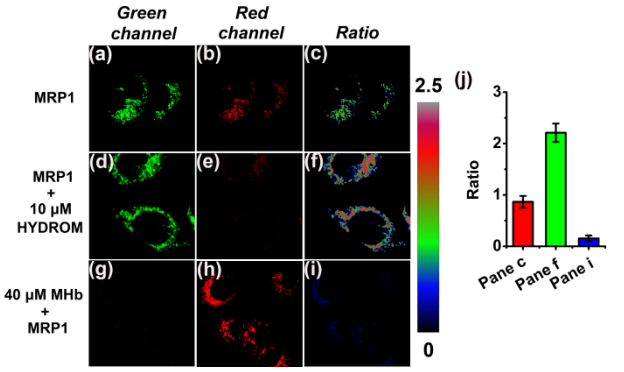

Fig. 5 Confocal image of endogenous mitochondrial HCN in PC12 cells. (a)-(c) Green (λ_{em} = 460-530 nm), red (λ_{em} = 575-650 nm) and ratiometric (F_{green} / F_{red}) imaging of PC12 cells incubated with **MRP1** (0.5 μ M). (d)-(f) Green, red, and ratiometric imaging of PC12 cells incubated with **MRP1** (0.5 μ M), and then incubated with 10 μ M HYDROM. (g)-(i) Green, red, and ratiometric imaging of PC12 cells pretreated with 40 μM MHb and then incubated with **MRP1** (0.5 μ M). (j) Average intensity ratios from images (c), (f), and (i). Error bars represent the standard deviations.

The above results provide support for the suggestion that probe **MRP1** may be used to detect different concentrations of endogenous HCN in PC12 cells. Due to the fast response time seen in the initial predicative studies discussed above, a further effort was made to test whether **MRP1** could be applied to visualize fluctuations in HCN levels in neurons. The neurons were differentiated from the neural stem cells as detailed in the Supporting Information. After incubating the neurons with **MRP1** for 15 min, the fluorescence ratio (F_{green} / F_{red}) was determined to be 0.89 (Fig. 6b). On this basis, the concentration of the endogenous HCN was calculated to be 8.4 μM. The cells were also stimulated with HYDROM (10 μM) for 15 min. Under these conditions, the fluorescence ratio increased to 2.09 (Fig. 6c). This value corresponds to an HCN concentration of 21.7 μM. When the HCN scavenger MHb (40 μM) was added to these cells, the fluorescence ratio immediately decreased to 0.18 (Fig. 6d). Thus, we suggest that **MRP1** can be used to monitor in real time variations in endogenous HCN concentrations within the mitochondria of neurons. To our knowledge this represents the first instance wherein a fluorescent probe is used to visualize endogenous HCN in nerve cells.

The cytotoxicity of **MRP1** in HepG2 cells was determined using a standard 3-(4,5-dimethylthiazol-2-yl)-2,5-diphenyl tetrazolium bromide (MTT) assay. On the basis of the results obtained, we infer that the low cytotoxicity of **MRP1** in live cells is relatively low (≥95% cell viability at a concentration of 5 μM; cf. Fig. S17).

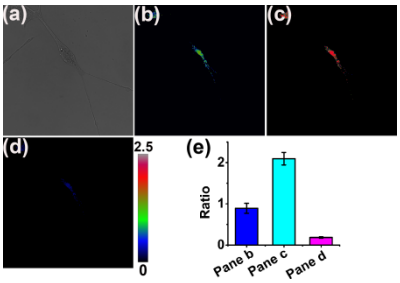

Fig. 6 Confocal image of endogenous mitochondrial HCN in neurons. (a) Bright field image. (b) Ratiometric (F_{green} / F_{red}) imaging of the neuron cells after incubation with **MRP1** (0.5 μ M) for 10 min. (c) Ratiometric (F_{green} / F_{red}) imaging of the cells in pane (b) and then further stimulated with HYDROM (10 μ M) for 10 min. (d) Ratiometric imaging of the cells in pane (c) that were then treated with MHb (40 μ M).

CONCLUSION

In summary, we have prepared and characterized a mitochondria-specific ratiometric fluorescence probe for HCN. This probe relies on 7-diethylamino-coumarin as the fluorophore, a 1-methylenepyrrolidinium group as the reactive cyanide recognition and mitochondria targeting subunit, and a benzyl chloride group to provide immobilization within mitochondria. Photophysical and spectral characterization studies revealed that a lead probe (**MRP1**) reacts rapidly (within 1 s) and responds reversibly to HCN with both high selectivity and sensitivity (the detection limit is 65.6 nM). Notably, probe **MRP1** is retained in the mitochondria even when the mitochondria membrane potential is decreased. It can be used to visualize different concentration of exogenous HCN within the mitochondria of HepG2 cells and proved effective in monitoring fluctuations in endogenous HCN concentrations within the mitochondria of PC12 Cells and neurons. It is thus believed that probe **MRP1** and related systems could emerge as useful tools that might allow the critical toxicological and physiological roles of HCN in human body to be understood in greater detail.

ASSOCIATED CONTENT

Supporting Information: Synthetic details, the method of cell culture and fluorescence imaging, and other spectroscopic data. This material is available free of charge via the Internet at http://pubs.acs.org.

AUTHOR INFORMATION

Corresponding Author

*sessler@cm.utexas.edu

Notes

The authors declare no competing financial interest.

ACKNOWLEDGMENT

The work in Austin was supported by the National Institutes of Health (RGM 103790A to J.L.S.) and the Robert A. Welch Foundation (F-0018). L. Long gratefully acknowledges the program of China Scholarships Council (201608320096 to L.L.) and the National Sciences Foundation of China (21202063 to L.L.) for financial support.

REFERENCES

(1) Baskin, S. I.; Brewer, T. G. Cyanide poisoning. In *Medical Aspects of Chemical and Biological Warfare*; Sidell, F., Takafuji, E. T.,Franz, D. R., Eds.; TMM Publication: Washington, DC, **1997**, p 271.

(2) Mokhlesi, B.; Leikin, J. B.; Murray, P.; Corbridge, T. C. *Chest* **2003**, *123*, 897.

(3) (a) Young, C.; Tidwell, L.; Anderson, C. *Cyanide: Social, Industrial, and Economic Aspects*; Minerals, Metals, and Materials Society: Warrendale, **2001**. (b) Long, L.; Wang, L.; Wu, Y.; Gong, A.; Da, Z.; Zhang, C.; Han, Z. *Chem. Asian J.* **2014**, *9*, 3291. (c) Zdor, R. E. *J. Appl. Microbiol.* **2015**, *118*, 267. (d) Ferrari, L. A.; Giannuzzi, L. *Forensic Sci. Int.* **2015**, *256*, 46. (e) Surleva, A. R.; Drochioiu, G. *J. Chem. Educ.* **2013**, *90*, 1654. (f) Moussa, S. G.; Leithead, A.; Li, S.-M.; Chan, T. W.; Wentzell, J. J. B.; Stroud, C.; Zhang, J.; Lee, P.; Lu, G.; Brook, J. R.; Hayden, K.; Narayan, J.; Liggio, J. *Atmos. Environ.* **2016**, *131*, 185. (g) Reade, M. C.; Davies, S. R.; Morley, P. T.; Dennett, J.; Jacobs, I. C.; Australian Resuscitation, C. *Emerg. Med. Australas* **2012**, *24*, 225.

(4) Way, J. L. *Annual Review of Pharmacology and Toxicology* **1984**, *24*, 451.

(5) Yamamoto, H.-a.; Mohanan, P. V. *Toxicology* **2002**, *179*, 29.

(6) (a) Prabhakaran, K.; Li, L.; Mills, E. M.; Borowitz, J. L.; Isom, G. E. *J. Pharmacol. Exp. Ther.* **2005**, *314*, 1338. (b) Sawa, A.; Wiegand, G. W.; Cooper, J.; Margolis, R. L.; Sharp, A. H.; Lawler, J. F.; Greenamyre, J. T.; Snyder, S. H.; Ross, C. A. *Nat. Med.* **1999**, *5*, 1194. (c) Dauer, W.; Przedborski, S. *Neuron* **2003**, *39*, 889. (d) McMillan, D. E.; Geevarghese, P. J. *Diabetes care* **1979**, *2*, 202. (e) Boland, M. L.; Chourasia, A. H.; Macleod, K. F. *Front. Oncol.* **2013**, *3*, 292.

(7) (a) Stelmaszynska, T.; Zgliczynski, J. The role of myeloperoxidase in phagocytosis, with special regard to HCN formation. In *Cyanide in Biology*; Vennesland, B., Conn, E., Knowles, C., Westley, J.,Wissing, F., Eds.; Academic Press: New York, **1981**, p 371. (b) Zgliczyński, J. M.; Stelmaszyńska, T. *Biochim. Biophys. Acta, Enzymology* **1979**, *567*, 309. (c) DeChatelet, L. R.; McPhail, L. C.; Shirley, P. S. *Blood* **1977**, *49*, 445.

(8) (a) Borowitz, J. L.; Gunasekar, P. G.; Isom, G. E. *Brain research* **1997**, *768*, 294. (b) Gunasekar, P.; Prabhakaran, K.; Li, L.; Zhang, L.; Isom, G.; Borowitz, J. *Neuroscience research* **2004**, *49*, 13. (c) Gunasekar, P. G.; Borowitz, J. L.; Turek, J. J.; Van Horn, D. A.; Isom, G. E. *J Neurosci Res* **2000**, *61*, 570. (d) Mills, E. M.; Gunasekar, P. G.; Pavlakovic, G.; Isom, G. E. *Journal of neurochemistry* **1996**, *67*, 1039.

(9) (a) Cipollone, R.; Visca, P. *IUBMB Life* **2007**, *59*, 187. (b) Cooper, C. E.; Brown, G. C. *J. Bioenerg. Biomembr.* **2008**, *40*, 533.

(10) (a) Yang, Y.; Zhao, Q.; Feng, W.; Li, F. *Chem. Rev.* **2013**, *113*, 192. (b) Chan, J.; Dodani, S. C.; Chang, C. J. *Nat. Chem.* **2012**, *4*, 973.

(11) Xu, Z.; Xu, L. *Chem. Commun.* **2016**, *52*, 1094.

(12) (a) Dong, Y. M.; Peng, Y.; Dong, M.; Wang, Y. W. *J. Org. Chem.* **2011**, *76*, 6962. (b) Gomez, T.; Moreno, D.; Diaz de Grenu, B.; Fernandez, A. C.; Rodriguez, T.; Rojo, J.; Cuevas, J. V.; Torroba, T. *Chem. Asian J.* **2013**, *8*, 1271. (c) Huang, X.; Gu, X.; Zhang, G.; Zhang, D. *Chem. Commun.* **2012**, *48*, 12195. (d) Kim, H. J.; Ko, K. C.; Lee, J. H.; Lee, J. Y.; Kim, J. S. *Chem. Commun.* **2011**, *47*, 2886. (e) Kumar, S.; Singh, P.; Hundal, G.; Hundal, M. S.; Kumar, S. *Chem. Commun.* **2013**, *49*, 2667. (f) Li, H.; Wen, Z.; Jin, L.; Kan, Y.; Yin, B. *Chem. Commun.* **2012**, *48*, 11659. (g) Lin, Y. D.; Pen, Y. S.; Su, W.; Liau, K. L.; Wen, Y. S.; Tu, C. H.; Sun, C. H.; Chow, T. J. *Chem. Asian J.* **2012**, *7*, 2864. (h) Lv, X.; Liu, J.; Liu, Y.; Zhao, Y.; Sun, Y. Q.; Wang, P.; Guo, W. *Chem. Commun.* **2011**, *47*, 12843. (i) Shankar, B. H.; Jayaram, D. T.; Ramaiah, D. *Chem. Asian J.* **2014**, *9*, 1636. (j) Yang, L.; Li, X.; Yang, J.; Qu, Y.; Hua, J. *ACS Appl. Mater. Interfaces* **2013**, *5*, 1317. (k) Zhang, P.; Shi, B.; You, X.; Zhang, Y.; Lin, Q.; Yao, H.; Wei, T. *Tetrahedron* **2014**, *70*, 1889. (l) Cho, D. G.; Kim, J. H.; Sessler, J. L. *J. Am. Chem. Soc.* **2008**, *130*, 12163. (m) Shiraishi, Y.; Nakamura, M.; Hayashi, N.; Hirai, T. *Anal. Chem.* **2016**, *88*, 6805. (n) Bejoymohandas, K. S.; Kumar, A.; Sreenadh, S.; Varathan, E.; Varughese, S.; Subramanian, V.; Reddy, M. L. *Inorg. Chem.* **2016**, *55*, 3448.

(13) (a) Divya, K. P.; Sreejith, S.; Balakrishna, B.; Jayamurthy, P.; Anees, P.; Ajayaghosh, A. *Chem. Commun.* **2010**, *46*, 6069. (b) Lee, J. H.; Jeong, A. R.; Shin, I. S.; Kim, H. J.; Hong, J. I. *Org. Lett.* **2010**, *12*, 764. (c) Xie, Y.; Ding, Y.; Li, X.; Wang, C.; Hill, J. P.; Ariga, K.; Zhang, W.; Zhu, W. *Chem. Commun.* **2012**, *48*, 11513. (d) Shojaeifard, Z.; Hemmateenejad, B.; Shamsipur, M. *ACS Appl. Mater. Interfaces* **2016**, *8*, 15177. (e) Kaushik, R.; Ghosh, A.; Singh, A.; Gupta, P.; Mittal, A.; Jose, D. A. *ACS Sensors* **2016**, *1*, 1265.

(14) (a) Liu, J.; Lin, Q.; Yao, H.; Wang, M.; Zhang, Y.-M.; Wei, T.-B. *Chin. Chem. Lett.* **2014**, *25*, 35. (b) Saha, S.; Ghosh, A.; Mahato, P.; Mishra, S.; Mishra, S. K.; Suresh, E.; Das, S.; Das, A. *Org. Lett.* **2010**, *12*, 3406. (c) Sharma, S.; Hundal, M. S.; Hundal, G. *Org. Biomol. Chem.* **2013**, *11*, 654.

(15) (a) Badugu, R.; Lakowicz, J. R.; Geddes, C. D. *J. Am. Chem. Soc.* **2005**, *127*, 3635. (b) Jamkratoke, M.; Ruangpornvisuti, V.; Tumcharern, G.; Tuntulani, T.; Tomapatanaget, B. *J. Org. Chem.* **2009**, *74*, 3919. (c) Kim, Y.; Huh, H. S.; Lee, M. H.; Lenov, I. L.; Zhao, H.; Gabbai, F. P. *Chem. Eur. J.* **2011**, *17*, 2057. (d) Varlan, M.; Blight, B. A.; Wang, S. *Chem. Commun.* **2012**, *48*, 12059.

(16) (a) Wang, L.; Zheng, J.; Yang, S.; Wu, C.; Liu, C.; Xiao, Y.; Li, Y.; Qing, Z.; Yang, R. *ACS Appl. Mater. Interfaces* **2015**, *7*, 19509. (b) Mannel-Croise, C.; Probst, B.; Zelder, F. *Anal. Chem.* **2009**, *81*, 9493. (c) Mannel-Croise, C.; Zelder, F. *ACS Appl. Mater. Interfaces* **2012**, *4*, 725.

(17) (a) Mello, J. V.; Finney, N. S. *Angew Chem Int Ed Engl* **2001**, *40*, 1536. (b) Kikuchi, K.; Takakusa, H.; Nagano, T. *TrAC, Trends Anal. Chem.* **2004**, *23*, 407.

(18) (a) Johnson, L. V.; Walsh, M. L.; Bockus, B. J.; Chen, L. B. *J Cell Biol* **1981**, *88*, 526. (b) Lemasters, J. J.; Qian, T.; Bradham, C. A.; Brenner, D. A.; Cascio, W. E.; Trost, L. C.; Nishimura, Y.; Nieminen, A.-L.; Herman, B. *J. Bioenerg. Biomembr.* **1999**, *31*, 305.

(19) Long, L. L.; Li, X. F.; Zhang, D. D.; Meng, S. C.; Zhang, J. F.; Sun, X. L.; Zhang, C.; Zhou, L. P.; Wang, L. *RSC Adv.* **2013**, *3*, 12204.

(20) Chen, Y.; Zhu, C.; Yang, Z.; Li, J.; Jiao, Y.; He, W.; Chen, J.; Guo, Z. *Chem. Commun.* **2012**, *48*, 5094.

(21) Bozdemir, O. A.; Sozmen, F.; Buyukcakir, O.; Guliyev, R.; Cakmak, Y.; Akkaya, E. U. *Org. Lett.* **2010**, *12*, 1400.

(22) Nag, A.; Chakrabarty, T.; Bhattacharyya, K. *J. Phys. Chem.* **1990**, *94*, 4203.

(23) (a) Guido, C. A.; Mennucci, B.; Jacquemin, D.; Adamo, C. *Phys. Chem. Chem. Phys.* **2010**, *12*, 8016. (b) Jacquemin, D.; Le Bahers, T.; Adamo, C.; Ciofini, I. *Phys. Chem. Chem. Phys.* **2012**, *14*, 5383.

(24) Presley, A. D.; Fuller, K. M.; Arriaga, E. A. *J. Chromatogr. B* **2003**, *793*, 141.

(25) (a) Dickinson, B. C.; Chang, C. J. *J. Am. Chem. Soc.* **2008**, *130*, 9638. (b) Zhou, R.; Yazdi, A. S.; Menu, P.; Tschopp, J. *Nature* **2011**, *469*, 221.

(26) Caporale, T.; Ciavardelli, D.; Di Ilio, C.; Lanuti, P.; Drago, D.; Sensi, S. L. *Exp. Neurol.* **2009**, *218*, 228.

(27) Moriya, F.; Hashimoto, Y. *Legal Med.* **2003**, *5*, S113.

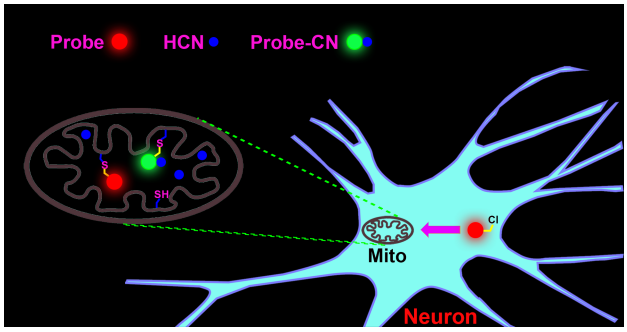

Graphical Abstract